Anisotropic analysis of trabecular architecture in human femur bone radiographs using quaternion wavelet transforms

S.Sangeetha[‡], C. M. Sujatha[♀] and D. Manamalli[‡]
[‡]Department of Instrumentation Engg, MIT Campus, Anna University, Chennai - 600 044, INDIA
[♀]Department of ECE, CEG Campus Anna University, Chennai - 600 025, INDIA
[‡]s.sangeethame@gmail.com (Corresponding author), [♀] sujathacm@annauniv.edu, manamalli_m@yahoo.com

Abstract— **In this work, anisotropy of compressive and tensile strength regions of femur trabecular bone are analysed using quaternion wavelet transforms. The normal and abnormal femur trabecular bone radiographic images are considered for this study. The sub-anatomic regions, which include compressive and tensile regions, are delineated using pre-processing procedures. These delineated regions are subjected to quaternion wavelet transforms and statistical parameters are derived from the transformed images. These parameters are correlated with apparent porosity, which is derived from the strength regions. Further, anisotropy is also calculated from the transformed images and is analyzed. Results show that the anisotropy values derived from second and third phase components of quaternion wavelet transform are found to be distinct for normal and abnormal samples with high statistical significance for both compressive and tensile regions. These investigations demonstrate that architectural anisotropy derived from QWT analysis is able to differentiate normal and abnormal samples.**

Keywords: Trabeculae; Radiographs; Quaternion wavelet transforms; Anisotropy; Apparent porosity

I. INTRODUCTION

The goal of biomechanics is to determine the changes of a given structural level, due to disease that affect the load carrying capacity of bone. Studies on correlation of structural features in human femur trabecular bone with mechanical variability are getting considerable interest [1]. Femur trabecular bone is porous type of bone with a complex dynamic structure. It is formed from a series of struts, giving rise to a structure in which there is a spatial variation of continuum level porosity and directionally dependent stiffness throughout the femur [2]. Its elastic and strength properties vary widely across anatomic sites, and with aging and disease. The trabeculae forms different patterns of net-like strands varying in thickness and number along the lines of maximum compression and tension stresses produced in the femur bone during load bearing conditions. These patterns are called as mechanical strength regions. Among all, the two important strength components are compressive and tensile groups. The compressive group is the thickest and most closely packed trabeculae in the upper end of the femur. Tensile group curves upward and inward across the neck of the femur, to end in the inferior portion of the femoral head [3, 4].

The biomechanical properties of trabecular bone depend not only on density but also on trabecular microarchitecture and mineralization. The most common method of assessing bone strength is to estimate loss of bone mass by Bone Mineral Densitometry. Bone mineral density (BMD) is a good surrogate for material property. Also characterization of the trabecular structural properties appears to be an important adjunct to the measurement of bone mass in determining fracture risk with greater accuracy [5]. The trabecular microstructure is typically oriented, such that it is organized along the lines of mechanical forces applied to bone. This microstructural directionality contributes to trabecular bone anisotropy [1]. The architectural deterioration caused by pathology results in alterations of structural anisotropy. Hence understanding of anisotropy of bone is important for diagnosis of osteoporosis like bone disorders.

Digital radiography is a widely available imaging modality that has the potential to reflect bone microarchitecture [6, 7]. X-ray imaging remains a very cost-effective technique, with many applications in both the medical and material science fields. The significant parts of the information that are available in 3D images are also available in the conventional radiograph [8]. Texture analysis has been increasingly used in image processing for identifying directional preferences of image features and provides more insight into bone structure. It yields localized information on a pixel level and is well suited to quantification of anisotropic properties in image data. Transforms have been used extensively in image processing for enhancement and for directional feature extraction. Quaternion algebra is found to be a powerful tool in analyzing orientation, shape, density and architecture of bone textures. The Quaternion Wavelet Transform (QWT) provides a quaternionic multiresolution analysis with 2D analytic wavelets. The quaternion magnitude-phase representation of the QWT is derived from Quaternion Fourier Transform (QFT) and consists of a real part and three imaginary parts. The first two QWT phases describe the shifts of the image features in the vertical and horizontal directions and the third QWT phase describe the texture information of the image [9]. The QWT has been applied to many fields such as image segmentation, edge detection and texture image classification [10].

In this work the anisotropy of trabecular architecture of strength regions is analyzed using multiscale QWT analysis. The compressive and tensile strength regions are delineated using pre-processing procedures. These delineated regions are subjected to quaternion wavelet transforms and statistical parameters are derived from the transformed images. These parameters are correlated with apparent porosity.

II. Methodology

Digitized femur images (N = 44) recorded using a clinical X-ray unit (Siemens 500mA Polyscope) are considered for this study. Two strength regions namely, compressive and tensile are identified manually by the position of the regions described in terms of a coordinate system whose axes comprised the shortest line across the femoral neck and a line through the center of the femoral head, the midpoint of the two axes as proposed by Singh delineation method [3]. The qualitative analysis is also performed on the delineated images to derive apparent porosity which is ratio of void area to bone area. The 2-D QWT depends on the quaternion 2-D Hilbert Transform and analytic signal. A quaternion may be represented in hypercomplex form as

$$q = a + bi + cj + dk \tag{1}$$

where a, b, c and d are real, i, j and k are complex operators. The quaternionic Fourier transform F^q of a real two-dimensional signal f is given by

$$F_A^q(\mu) = (1 + \mathrm{sgn}(u))(1 + \mathrm{sgn}(v))F^q(\mu) \tag{2}$$

where $\mu = (u, v)$. This can be expressed in the spatial domain as follows

$$F_A^q(x) = f(x) + n^T f_{Hi}(x) \tag{3}$$

where $n^T = (i, j, k)^T$ and f_{Hi} is a vector which consists of the total and the partial Hilbert transforms of [11]. The analytic wavelets of 2D signal are constructed by setting its Hilbert transform in the imaginary part [12, 13]. The analytic extension of mother wavelets ψ^D , ψ^V , ψ^H and scaling function φ are given as

$$\begin{aligned}
\psi^D(x,y) &= \psi_h(x)\psi_h(y) \rightarrow \psi^D + iH_{i1}\psi^D + jH_{i2}\psi^D + kH_i\psi^D \\
\psi^V(x,y) &= \phi_h(x)\psi_h(y) \rightarrow \psi^V + iH_{i1}\psi^V + jH_{i2}\psi^V + kH_i\psi^V \\
\psi^H(x,y) &= \psi_h(x)\phi_h(y) \rightarrow \psi^H + iH_{i1}\psi^H + jH_{i2}\psi^H + kH_i\psi^H \\
\phi(x,y) &= \phi_h(x)\phi_h(y) \rightarrow \phi + iH_{i1}\phi + jH_{i2}\phi + kH_i\phi
\end{aligned} \tag{4}$$

where H_{i1}, H_{i2} are partial Hilbert transform along x and y axis respectively, H_i is combination of two partial Hilbert transforms along both axes. The 2D Hilbert transform of separable functions is equivalent to 1D Hilbert transform along rows and columns.

The 1D Hilbert pair of wavelets and scaling functions are given by $(\psi_h, \psi_g = H\psi_h)(\phi_h, \phi_g = H\phi_h)$. The quaternion wavelets are represented in terms of separable products and are given by

$$\begin{aligned}
\psi^D(x,y) &= \psi_h(x)\psi_h(y) + i\psi_g(x)\psi_h(y) + j\psi_h(x)\psi_g(y) + k\psi_g(x)\psi_g(y) \\
\psi^V(x,y) &= \phi_h(x)\psi_h(y) + i\phi_g(x)\psi_h(y) + j\phi_h(x)\psi_g(y) + k\phi_g(x)\psi_g(y) \\
\psi^H(x,y) &= \psi_h(x)\phi_h(y) + i\psi_g(x)\phi_h(y) + j\psi_h(x)\phi_g(y) + k\psi_g(x)\phi_g(y) \\
\phi(x,y) &= \phi_h(x)\phi_h(y) + i\phi_g(x)\phi_h(y) + j\phi_h(x)\phi_g(y) + k\phi_g(x)\phi_g(y)
\end{aligned} \tag{5}$$

Each quaternion wavelet basis contains four components in the vertical, horizontal and both directions, which are of 90 degree phase shift with each other. Statistical features which include mean, standard deviation, kurtosis, skewness and energy are extracted for the QWT approximation, horizontal, vertical and diagonal components. Anisotropy is estimated out of phase images that are derived from quaternion analysis.

Eigenvalue I (λ_1), Eigenvalue II (λ_2) and Eigenvalue III (λ_3) are calculated for all the transformed images extracted from the QWT approximation, horizontal, vertical and diagonal components. Further from these Eigen values, anisotropy, relative and fractional anisotropy are derived.

$$RA = \sqrt{\frac{1}{3}}\frac{\sqrt{(\lambda_1 - (\lambda))^2 + (\lambda_2 - (\lambda))^2 + (\lambda_3 - (\lambda))^2}}{(\lambda)} \tag{6}$$

$$FA = \sqrt{\frac{3}{2}}\frac{\sqrt{(\lambda_1 - (\lambda))^2 + (\lambda_2 - (\lambda))^2 + (\lambda_3 - (\lambda))^2}}{\sqrt{\lambda_1^2 + \lambda_2^2 + \lambda_3^2}} \tag{7}$$

FA represents anisotropic diffusion weighted against total diffusion [14]. Thus anisotropy parameters are derived and are correlated with apparent porosity.

III. Results and Discussion

The typical binarized planar radiographic images of normal and abnormal femur trabecular bone are shown in Fig.1 (a) and (b) respectively. In normal images, it is observed that all the trabecular patterns are distinct and are closely arranged

and in abnormal, spacing is more with high discontinuities. The apparent porosity is found to be low for normal and high in case of abnormal bones in both the regions.

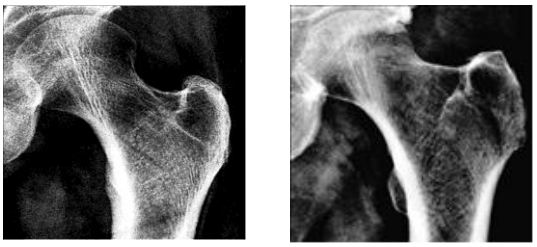

(a) (b)

Figure. 1. Representative images (a) normal and (b) abnormal femur bone

The variations of QWT features with apparent porosity for three different phase components are shown in Fig. 2 (a), (b) and (c) respectively. The variations of kurtosis derived from the phase components are high for normal and low for abnormal subjects. This could be due to randomness of variations in the structure caused by pathology affecting these regions. These values are widely scattered for first phase component and are less scattered for second phase component in both the subjects. Also these values vary linearly with apparent porosity for third phase component and have a high correlation. The first and second phase components yield information about the spatial location whereas third phase component yield coherent description of local structures. Hence, this shows that the quaternionic third phase component is able to extract the structural variations of patterns in compressive region. The difference in these values between normal and abnormal images is statistically highly significant for all the phase components. This shows the ability of this feature to discriminate normal and abnormal bones.

The anisotropy measure obtained from phase components in horizontal, vertical and diagonal subbands of QWT is presented in Table 1. In the case of horizontal subband, anisotropy values obtained from the first phase component are high for abnormal subjects which may be due to heterogeneous and complex biomechanical behaviour of bones. The anisotropic values derived from third phase component are found to be very low indicating that it captures trabecular pattern of non-uniform variation. The anisotropy index values derived from second phase components are found to be high and distinct in normal and abnormal samples. Hence it appears that these index values could be used as discriminative measure.

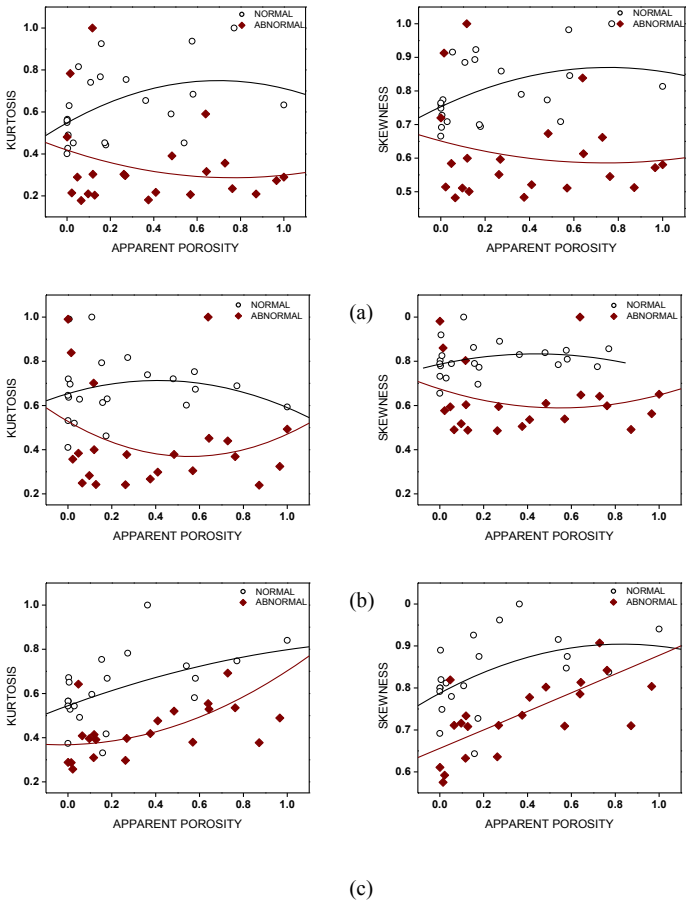

Figure.2. Variations of kurtosis and skewness with apparent porosity for (a) first, (b) second and (c) third phase components of normal and abnormal samples in compressive strength regions.

TABLE I. ANISOTROPY VALUES OF PHASE COMPONENTS IN HORIZONTAL, VERTICAL AND DIAGONAL SUBBAND

Subbands		FA			RA			AI		
		P_1	P_2	P_3	P_1	P_2	P_3	P_1	P_2	P_3
Horizontal	Normal	0.34	0.73	0.24	0.21	0.56	0.17	0.34	0.68	0.24
	Abnormal	0.38	0.70	0.26	0.27	0.53	0.15	0.36	0.66	0.25
Vertical	Normal	0.69	0.38	0.24	0.52	0.24	0.14	0.65	0.36	0.24
	Abnormal	0.67	0.34	0.24	0.52	0.23	0.14	0.63	0.32	0.24
Diagonal	Normal	0.33	0.37	0.24	0.21	0.24	0.14	0.33	0.35	0.23
	Abnormal	0.38	0.33	0.20	0.28	0.23	0.12	0.36	0.32	0.19

The first phase component of vertical subband yields high values of FA, RA and AI in both normal and abnormal subjects. Among all the anisotropy values, FA is found to be high which shows pronounced anisotropic distribution. The anisotropy measure obtained from phase components of diagonal subband are found to have low magnitude when compared to other subbands. This represents the

heterogeneity of trabecular patterns. The anisotropy values derived from second phase components are found to be high and distinct in normal and abnormal samples. Similar was the analysis in tensile region.

IV. Conclusion

The evaluation of bone quality plays an important role in the diagnosis of bone disorders and can improve the prediction rate of fracture risk. Bone mineral density is considered clinically essential in explaining the mechanical variability of bone. However, it has been acknowledged that the role of bone structure is as important in the determination of bone quality as bone mineral density [15]. The compressive and tensile strength regions are delineated using pre-processing procedures. These delineated regions are subjected to quaternion wavelet transforms and statistical parameters are derived from the transformed images. The anisotropy values are also determined from these transformed images. The qualitative analysis is performed on the delineated images to derive apparent porosity. The parameters derived from the transformed images are correlated with apparent porosity and are found to be statistically significant for both compressive and tensile regions. Results show that the anisotropy values derived from second and third phase components of quaternion wavelet transform are found to be distinct for normal and abnormal samples. These investigations demonstrate that architectural anisotropy derived from QWT analysis is able to differentiate normal and abnormal samples. This automated analysis can be used to enhance the diagnosis without much human intervention, which would be useful for mass screening of osteoporosis and bone mass disorders.

References

[1] T. M. Keaveny, E. F. Morgan, G. L. Niebur and O. C. Yeh, "Biomechanics of trabecular bone," *Annual Review of Biomedical Engineering*, vol. 3, pp. 307-333, 2001.

[2] T. M. Andrew, "Structural Optimisation: Biomechanics of the Femur," *Engineering and Computational Mechanics*, vol. 165, pp. 1286, 2012

[3] M. Singh, A. R. Nagrath and P. S. Maini, "Changes in trabecular pattern of the upper end of the femur as an index of osteoporosis," Journal of Bone and Joint Surgery, vol. 52, no. 3, pp. 457-467, 1970

[4] P. P. Smyth, J. E. Adams, R. W. Whitehouse and C. J. Taylor, "Application of computer texture analysis to the Singh index," *The British Journal of Radiology*, vol. 70, no. 831, pp. 242-247, 1997

[5] G. Diederichs, T. M. Link, M. Kentenich, K. Schwieger, M. B. Huber, A. J. Burghardt and A. S. Issever, "Assessment of trabecular bone structure of the calcaneus using multi-detector CT: correlation with micro CT and biomechanical testing," *Bone*, vol. 44, no.5, pp. 976-983, 2009.

[6] L. T. Corroller, J. Halgrin, M. Pithioux, D. Guenoun, P. Chabrand and P. Champsaur, "Combination of texture analysis and bone mineral density improves the prediction of fracture load in human femurs," *Osteoporosis International*, vol. 23, no. 1, pp. 163-169, 2012

[7] L. Pothuaud, P. Carceller and D. Hans D, "A Correlations between grey-level variations in 2D projection images (TBS) and 3D microarchitecture: Applications in the study of human trabecular bone microarchitecture," *Bone*, vol. 42, no. 4, pp.775-787, 2008

[8] P. D. Delmas and E. Seeman, "Changes in bone mineral density explain little of the reduction in vertebral or nonvertebral fracture risk with anti-resorptive therapy," *Bone*, vol. 34, no. 4, pp. 599-604, 2004

[9] R. Soulard and P. Carre, "Quaternionic Wavelets for Texture Classification," *Pattern Recognition Letters* 32, vol.13, pp.1669-1678, 2004

[10] S. Gai, G. Yang and M. Wan, "Employing quaternion wavelet transform for bank note classification," *Neurocomputing*, vol. 1, no. 18, pp. 171–178, 2013

[11] L. H. Qiao, W. Guo, W. Yuan, W. Niu and L. Peng, "Texture analysis based on bidimensional empirical mode decomposition and quaternions," *Proceedings of the International Conference on Wavelet Analysis and Pattern Recognition*, pp. 84-90, 2012

[12] Y, Xu, "Quaternion-based discriminant analysis method for color face recognition," *Plos One*, vol. 7, no. 8, pp. 1-4, 2012

[13] M. Yin, W. Liu, J. Shui and J. Wu, "Quaternion Wavelet Analysis and Application in Image Denoising," *Mathematical Problems in Engineering*, vol. 20, pp.1-21, 2012.

[14] M. D. Budde and J. A. Frank, "Examining brain microstructure using structure tensor analysis of histological sections," *NeuroImage*, vol. 63, pp. 1–10, 2012

[15] W. L. Roque, K. Arcaro and A. Alberich-Bayarri, "Mechanical competence of bone: A new parameter to grade trabecular bone fragility from tortuosity and elasticity," *IEEE Transactions on Biomedical Engineering*, vol. 60, no. 5, pp. 1363-1370, 2013